

Predicting the aggregation stability of nanostructures based on polyVCL-polyVI copolymers: mesoscopic simulation

M.K. Glagolev, Ya.N. Shatskaya, A.V. Vorozheykina, A.I. Barabanova, P.V. Komarov
A.N. Nesmeyanov Institute of Organoelement Compounds of RAS, Moscow, Russia
pv_komarov@mail.ru

DOI: 10.26456/pcascnn/2025.17.374

Abstract: Computer simulation of the aggregation behavior of thermosensitive copolymers of *N*-vinylcaprolactam (*VCL*) and *N*-vinylimidazole (*VI*) was performed in the framework of a coarse-grained model. Virtual synthesis of the copolymers from a monomer feed with different compositions was implemented using a Kinetic Monte Carlo method. At low conversions, statistical copolymers were obtained, while at high conversions, the copolymers contained a long block of *VCL* units. The aggregation behavior of the constructed copolymers was studied using Langevin dynamics in the solvent environment that is poor for the *VCL* units, which, in terms of the devised model, corresponds to the temperatures above the lower critical solution temperature for the *VCL*. It was shown that the aggregation of *VCL* blocks initially leads to the formation of nanoparticle-like nanostructures with a core-shell morphology, where the core is formed by *VCL* blocks and the shell is formed by *VI* blocks. The presence of a homopolymer *VCL* block increases the density of the core, while its length and the *VCL* content in the monomer feed affect the size of the shell. It was shown that the nanostructures formed at $f_{VCL} = 0,55$ (*VCL* content in the monomer feed) have the highest aggregation stability. In this case, when the solvent is poor for the *VCL*, the mesoglobules are formed, consisting on average of 2-3 polymer chains. The polymers produced from monomer feed with higher *VCL* content form potentially aggregation-unstable nanostructures. Also, the polymers obtained at $f_{VCL} = 0,55$ have the highest specific solvent-accessible area of *VI* units, which makes them a prospective basis for the development of thermally-switched catalysts.

Keywords: poly(*N*-vinylcaprolactam), poly(*N*-vinylimidazole), thermosensitive copolymers, computer simulation, thermally-switched catalysts.

Mikhail K. Glagolev – Ph. D., Researcher, Laboratory of Physical Chemistry of Polymers, A.N. Nesmeyanov Institute of Organoelement Compounds of RAS, ORCID: 0000-0003-1128-649X

Yaroslava N. Shatskaya – Senior Laboratory Assistant, Laboratory of Physical Chemistry of Polymers, A.N. Nesmeyanov Institute of Organoelement Compounds of RAS, ORCID: 0009-0006-7497-6454

Alesya V. Vorozheykina – Junior Researcher, Laboratory of Physical Chemistry of Polymers, A.N. Nesmeyanov Institute of Organoelement Compounds of RAS, ORCID: 0000-0002-0919-7458

Anna I. Barabanova – Ph. D., Senior Researcher, Laboratory of Physical Chemistry of Polymers, A.N. Nesmeyanov Institute of Organoelement Compounds of RAS, ORCID: 0000-0001-7016-1422

Pavel V. Komarov – Dr. Sc., Docent, Leading Researcher Laboratory of Physical Chemistry of Polymers, A.N. Nesmeyanov Institute of Organoelement Compounds of RAS, ORCID: 0000-0003-2138-5088

УДК 544.23.022

Оригинальная статья

Прогнозирование агрегативной устойчивости наноструктур на основе сополимеров полиВКЛ-полиВИ: мезоскопическое моделирование

М.К. Глаголев, Я.Н. Шатская, А.В. Ворожейкина, А.И. Барабанова, П.В. Комаров
ФГБУН «Институт элементоорганических соединений им. А.Н. Несмеянова РАН»
119991, Россия, Москва, ул. Вавилова, 28б

DOI: 10.26456/pcascnn/2025.17.374

Аннотация: В рамках крупнозернистого моделирования выполнено изучение агрегационной стабильности термочувствительных сополимеров на основе *N*-винилкапролактама (ВКЛ) и *N*-винилимидазола (ВИ). Виртуальный синтез сополимеров различного состава был выполнен с использованием кинетического метода Монте-Карло. При малых степенях конверсии были получены статистические сополимеры, в то время как при высоких степенях конверсии построенные сополимеры содержали длинный гомополимерный ВКЛ-блок. Агрегационные свойства полученных сополимеров были изучены в рамках динамики Ланжевена в среде

© М.К. Glagolev, Ya.N. Shatskaya, A.V. Vorozheykina, A.I. Barabanova, P.V. Komarov, 2025

растворителя, которая является неблагоприятной для сомономеров ВКЛ, что, согласно разработанной модели, соответствует температурам, превышающим нижнюю критическую температуру растворения для поли-ВКЛ. Было показано, что агрегация ВКЛ-блоков первоначально приводит к образованию наночастиц с морфологией ядро-оболочка, где ядро образовано блоками на основе ВКЛ, а оболочка образована блоками ВИ. Наличие гомополимерного ВКЛ-блока увеличивает плотность ядра, в то время как его длина и содержание мономеров ВКЛ в реакционной смеси — на размер оболочки. Было показано, что наноструктуры, образованные, когда доля ВКЛ в реакционной смеси равна $f_{VCL}=0,55$, обладают наибольшей агрегационной стабильностью. В этом случае, когда растворитель является плохим для ВКЛ, образуются мезоглобулы, содержащие в среднем из 2-3 полимерных цепочек. Полимеры, полученные из реакционной смеси с более высоким содержанием ВКЛ, образуют потенциально агрегационно нестабильные наноструктуры. Кроме того, полимеры, полученные при $f_{VCL}=0,55$, имеют самую высокую удельную площадь, доступную для растворителя, что делает их перспективной основой для разработки термочувствительных катализаторов.

Ключевые слова: поли(*N*-винилкапролактан), поли(*N*-винилимидазол), термочувствительные сополимеры, компьютерное моделирование, катализаторы с термическим переключением.

Глаголев Михаил Константинович – к.ф.-м.н., научный сотрудник лаборатории физической химии полимеров ФГБУН «Институт элементоорганических соединений им. А.Н. Несмеянова РАН»

Шатская Ярослава Николаевна – старший лаборант лаборатории физической химии полимеров ФГБУН «Институт элементоорганических соединений им. А.Н. Несмеянова РАН»

Ворожейкина Алеся Витальевна – к.ф.-м.н., младший научный сотрудник лаборатории физической химии полимеров ФГБУН «Институт элементоорганических соединений им. А.Н. Несмеянова РАН»

Барабанова Анна Ивановна – к.х.н., старший научный сотрудник лаборатории физической химии полимеров ФГБУН «Институт элементоорганических соединений им. А.Н. Несмеянова РАН»

Комаров Павел Вячеславович – д.ф.-м.н., доцент, ведущий научный сотрудник лаборатории физической химии полимеров ФГБУН «Институт элементоорганических соединений им. А.Н. Несмеянова РАН»

Поступила в редакцию/received: 18.07.2025; после рецензирования/reviced: 02.09.2025; принята/accepted: 09.09.2025.

1. Introduction

Stimuli-responsive polymers are a class of molecular systems that can undergo reversible nanoscale structural transitions, changing their physical and chemical properties as a response to external conditions, such as temperature, radiation, pH of the solution, etc. [1]. Understanding these processes is the key to directed development of functional materials for sensors, tunable surfaces, nanocontainers and other applications [2-4], such as thermo-switchable catalysts [5-7]. The latter can be based on thermosensitive polymers with lower critical solution temperature (LCST) [8-10].

Our work is devoted to the study of nanostructures that are formed in aqueous solutions of copolymer synthesized from *N*-vinylcaprolactam (*VCL*) and *N*-vinylimidazole (*VI*). The *VCL* units endow the copolymers, which are hydrophilic at normal conditions, with thermal sensitivity. The value of their LCST can be adjusted by varying their molecular mass characteristics [11], allowing to tune their reversible conformational transition. The polar *VI* units, in their turn, are able to coordinate [12-14] with metal ions, imparting the catalytic activity to the copolymers. This allows us to consider these copolymers as a prospective basis for thermo-switchable catalysts [15] and makes studying them an important task.

The bulk radical copolymerization of *VCL* and *VI* was implemented in our previous experimental research [16-18]. It was found that the copolymers maintain constant composition until the more reactive *VI* units in the monomer feed are exhausted. The monomer unit distribution in the polymer can be controlled by the composition of the monomer feed and the reaction duration. This was corroborated by the Kinetic Monte-Carlo (KMC) model under the assumption that the monomer unit concentrations around the reaction centers are quasi-stationary [18]. Experimental study of the copolymers revealed a conformational transition with the formation of mesoglobules. The coil-to-globule transitions were also observed in Langevin dynamics simulations [18]. However, these simulations were performed only for solitary macromolecules, which doesn't allow assessing the structure of mesoglobules observed in the experiments. This work aimed to study the aggregation behavior of the virtually synthesized *VCL-VI* copolymers and the structure of their aggregates. The simulations were performed using the workflow introduced in our previous study [18].

2. The object of the research

We consider the heterogeneous multi-block copolymers of *N*-vinylcaprolactam and *N*-vinylimidazole, synthesized *in silico* from monomer feed of various compositions. In terms of the KMC model, the latter were determined by the molar fraction of the *VCL* monomers f_{VCL} , which was equal to 0,55, 0,7 and 0,85. The monomer to initiator ratio was fixed at 500:1, resulting in an average degree of polymerization $N = 500$ at full conversion. As it was shown in [18], the synthesized copolymer consists of alternating *VCL* and *VI* blocks of random length (the statistical block) and a long homopolymer *VCL* block (*PVCL* block) formed after the *VI* units in the monomer feed are consumed.

The length of the *PVCL* block can be controlled by stopping the reaction at a particular time. The copolymers were characterized by the total length of the polymer chain N , the number of monomer units in the *PVCL* tail N_{tail} , and the relative length of the *PVCL* block $l_{tail} = N_{tail} / N$. In our study, we consider the chains with $l_{tail} = 0; 0,125; 0,25$ and the chains obtained by full conversion of the monomers in the monomer feed (named hereafter as «full chains»). For the monomer feed with $f_{VCL} = 0,55$, the «full» chains correspond to $l_{tail} = 0,444$, at $f_{VCL} = 0,7$ the value is $l_{tail} = 0,564$, and for $f_{VCL} = 0,85$ the value is $l_{tail} = 0,683$. The average lengths of the *VCL* blocks b_{VCL} and *VI* blocks b_{VI} in the statistical block of the copolymer were $b_{VCL} = 1,2$ and $b_{VI} = 5,4$ at $f_{VCL} = 0,55$; $b_{VCL} = 1,4$ and $b_{VI} = 3,1$ at $f_{VCL} = 0,7$; $b_{VCL} = 2,0$ and $b_{VI} = 2,0$ at $f_{VCL} = 0,85$.

3. The model and simulation technique

The detailed description of the model is available in the supporting information for our recent study [18]. The monomer sequences were generated using the KMC method by sequentially joining randomly chosen monomer units from a virtual reactor to growing polymer chains. The probabilities of joining depended on the types of the terminal unit of the chain and the unit about to join the chain. They were chosen according to experimentally determined reactivities of the monomers. According to the experimental data, the concentrations of the monomer units near the reaction center were assumed constant up to the point where the more reactive *VI* was fully consumed.

The aggregation behavior and the structure of the copolymers were studied using the Langevin dynamics with a Kremer-Grest type model [19]. The model parameters are provided in terms of dimensionless Lennard-Jones units. Each monomer unit was represented by a structureless spherical particle with a diameter of $\sigma = 1$. The excluded volume interactions were represented by the repulsive part of the Lennard-Jones potential:

$$U_{ev} = 4\varepsilon \left((\sigma/r)^{12} - (\sigma/r)^6 \right) + 1/4, \quad r < r_c, \quad (1)$$

where $r_c = 2^{1/6}\sigma$ is the cutoff radius. The implicit solvent environment was represented by the Yukawa-type attractive potential between the *VCL* units:

$$U_{solv} = A \left(\exp(-kr_{ij})/r_{ij} - \exp(-kr_{solv})/r_{solv} \right), \quad r < r_{solv}, \quad (2)$$

where the cutoff radius is $r_{solv} = 4\sigma$, and the exponential decay parameter is $k = 0,23$, and the factor A controls the solvent quality. The lengths of the bonds between the monomer units $b = 1\sigma$ were maintained very close to $b = 1$ by a harmonic potential:

$$U_{bond} = K_{bond} (l - b), \quad (2)$$

where l is the actual bond length, $K_{bond} = 10000$. The temperature of the system $T = 1$ was maintained by a Langevin thermostat.

The initial chain configurations were created by the Mouse2 package [20] using the monomer sequences from the KMC model. They were placed in cubic simulation cells with an edge $a = 1000\sigma$ and periodic boundary conditions (infinitely dilute solution) and equilibrated for 2×10^5 time units τ with $A = 0$. The A was then changed with a step of $\Delta A = -0,01$ every $10^4 \tau$ until it reached $A = 2$, causing formation of nanostructured aggregates. To study the aggregation stability, the latter were cloned and placed in the nodes of a cubic lattice with dimensions $n \times n \times n$ ($n = 2$ or 3) in the simulation cell with periodic boundary conditions and edge size $2nD_g\sigma$, where D_g is the size of the globules.

The prepared solutions were simulated for $2 \times 10^6 \tau$, with the final $5 \times 10^5 \tau$ used to collect the data. The separate aggregates (mesoglobules) were distinguished using the Mouse2 cluster analysis routine [20], and their

aggregation numbers N_{aggr} (the number of individual chains forming an aggregate) were calculated. The accessibility of the VI units in the aggregates to the solvent was analyzed by calculating the specific solvent-accessible surface area (SASA) of the VI units using the method described in Ref. [21]. The diameters of the monomer units were taken as $d_{VCL} = d_{VI} = \sigma$, the probe radius was taken as $r_{probe} = 0,5\sigma$.

4. Results of simulations

The simulation of solitary chains has shown that deterioration of the solvent quality leads to the coil-to-globule transition in the copolymer, with the VCL units forming dense aggregates. The aggregate sizes depend on the quantity of the VCL units and increase along with both f_{VCL} and l_{tail} . The VI blocks within the statistical block of the copolymer form loops around the dense VCL aggregates. When a single VCL aggregate is formed, the nanostructures can be classified as belonging to the «core-shell» type.

Table 1. Average aggregation number $\langle N_{aggr} \rangle$ depending on the VCL units fraction in the monomer feed f_{VCL} , and the ratio of $PVCL$ block length and total chain length l_{tail} . The aggregation-stable systems are designated with «S», and the aggregation-unstable ones with «U».

f_{VCL}/l_{tail}	0	0,125	0,25	0,375	full*
0,55	2,1 (S)	2,0 (S)	3,0 (S)	2,1 (S)	3,6 (S)
0,7	11,5(S)	13,5(S)	13,5(S)	27* (U)	27* (U)
0,85	27*(U)	(U)	(U)	(U)	27*(U)

The aggregation stability of the obtained systems was then studied. Table 1 contains average aggregation numbers $\langle N_{aggr} \rangle$, equal to the average number of polymer chains in one aggregate. The values $\langle N_{aggr} \rangle = n^3$ show that all of the polymer chains in the system eventually compose a single aggregate, indicating aggregation instability. As one can see from Table 1, an increase in both f_{VCL} and l_{tail} leads to an increase in the average aggregate size. For systems with $f_{VCL} = 0,55$ it is $\langle N_{aggr} \rangle = 2...3,6$ for all values of l_{tail} . This is much smaller than the total number of molecules in the system, indicating aggregation stability. The snapshots of the systems with $f_{VCL} = 0,55$, and, $l_{tail} = 0,45$ are shown in fig. 1 a, b. One can see that the presence of a $PVCL$ block leads to the formation of much larger aggregates with a dense core of the VCL units in the center of aggregates (see fig. 1 b). At $f_{VCL} = 0,7$, large mesoglobules are formed (see fig. 1 c). Unlike the spherical mesoglobules observed at $f_{VCL} = 0,55$, these globular nanostructures have an elongated shape. Their morphology is typical

for random copolymers enriched with solvophilic units [22-24]. Further increase of the VCL content in the macromolecules leads to an increase in the aggregate size. For systems with $f_{VCL} = 0,7$ at full monomer conversion, as well as for all of the systems with $f_{VCL} = 0,85$, all macromolecules aggregated together, meaning aggregation instability.

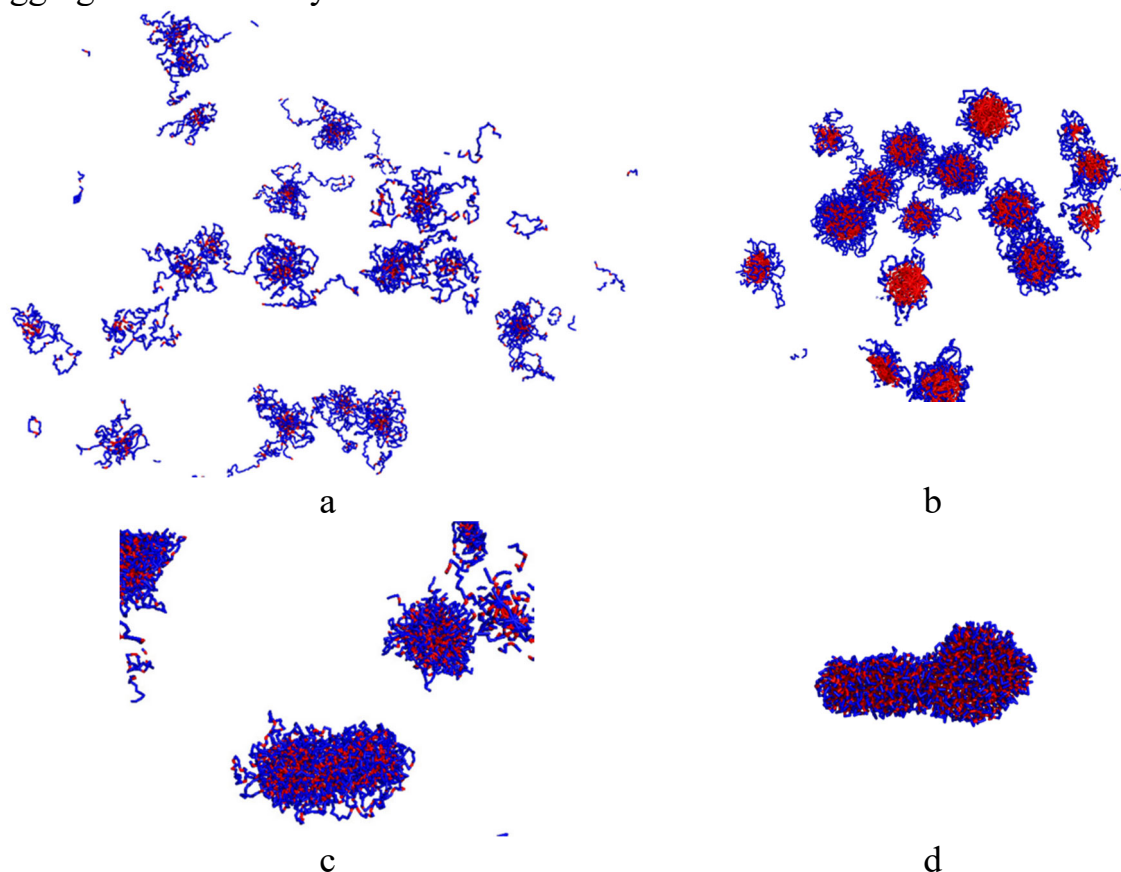


Fig. 1. The snapshots of the systems with $n = 27$ when: (a) $f_{VCL} = 0,55$, $l_{tail} = 0$; (b) $f_{VCL} = 0,55$, $l_{tail} = 0,45$; (c) $f_{VCL} = 0,7$, $l_{tail} = 0$; (d) $f_{VCL} = 0,85$, $l_{tail} = 0$. The VCL monomer units are colored red, the VI units are colored blue.

It should be noted that while in aggregation-stable systems the average number of aggregates stays constant after equilibration, the aggregates can stick together and split in the course of the simulation.

A more detailed insight into the aggregation behavior is possible by analyzing the distributions of the aggregate sizes (see fig. 2). One can see that, except for $f_{VCL} = 0,55$ and $l_{tail} = 0,375$, an increase of both f_{VCL} and l_{tail} leads to a wider mass distribution of the aggregates. In the systems with $f_{VCL} = 0,55$ and $l_{tail} \leq 0,125$, some chains are not included in the aggregates ($N_{aggr} = 1$). For $f_{VCL} = 0,55$ and $l_{tail} \leq 0,375$, the highest mass fraction corresponds to the aggregates formed by 2 chains. For chains synthesized at $f_{VCL} = 0,55$ and full conversion of monomer ($l_{tail} = 0,444$), most of the aggregates consist of 2 or 3 polymer chains,

while larger aggregates with N_{aggr} up to 15 keep forming and disintegrating in the solution. At $f_{VCL} = 0,7$, stable aggregates with a size of $N_{aggr} = 19$ are formed, which are not observed at $f_{VCL} = 0,55$.

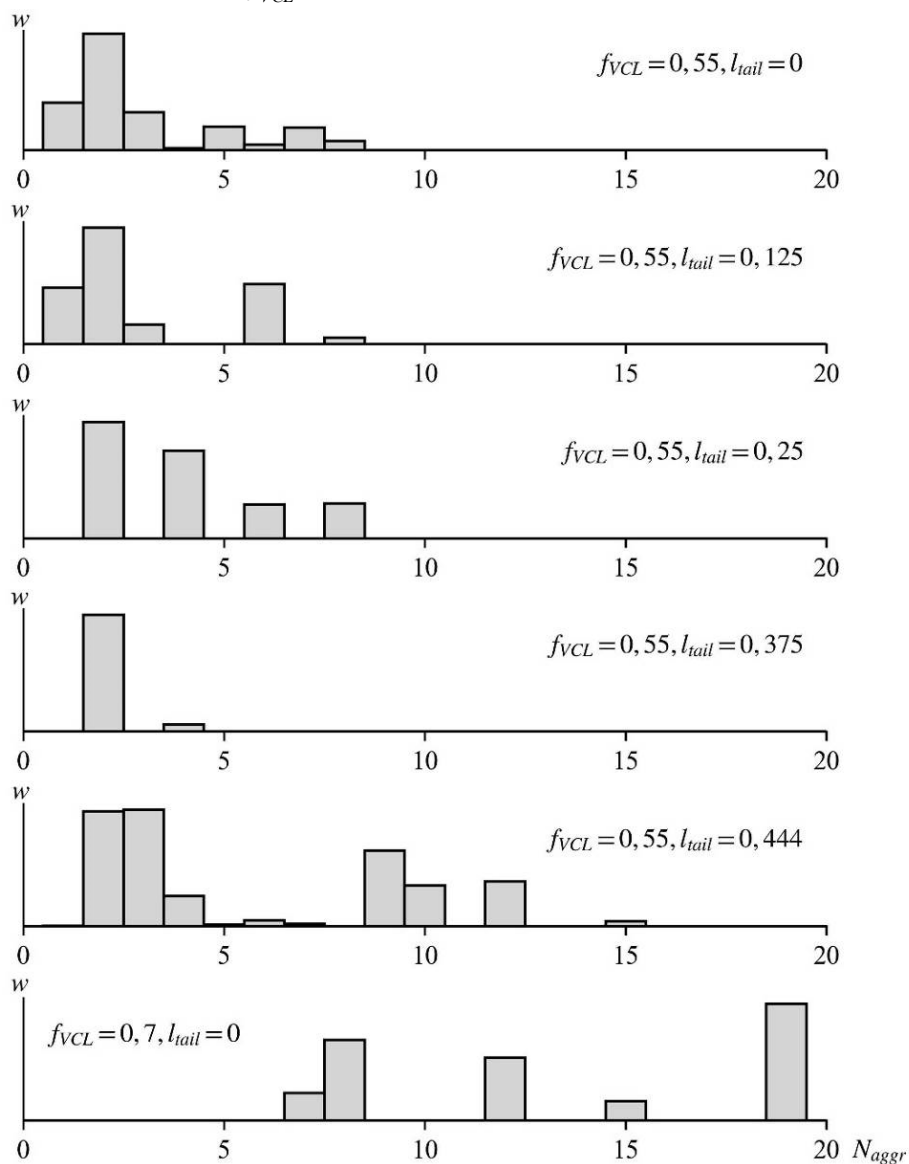


Fig. 2. Distributions of masses of aggregates of macromolecules with different f_{VCL} and l_{tail} depending on their aggregation numbers.

To describe the structure of aggregates, a quantitative assessment of accessibility of the VI units for the solvent was performed by calculating specific SASA for the VI units S_{VI} . The results were averaged between aggregates having a specified aggregation number, N_{aggr} . As one can see in fig. 3, the highest S_{VI} is observed in the system with $f_{VCL} = 0,55$, $l_{tail} = 0$. Here, the S_{VI} is around 4,5 and is almost independent of the aggregate size. This confirms the visual observation that the VI units form loops surrounded by the solvent, so that the S_{VI} value is close to that expected for a cylinder with a diameter of 1σ .

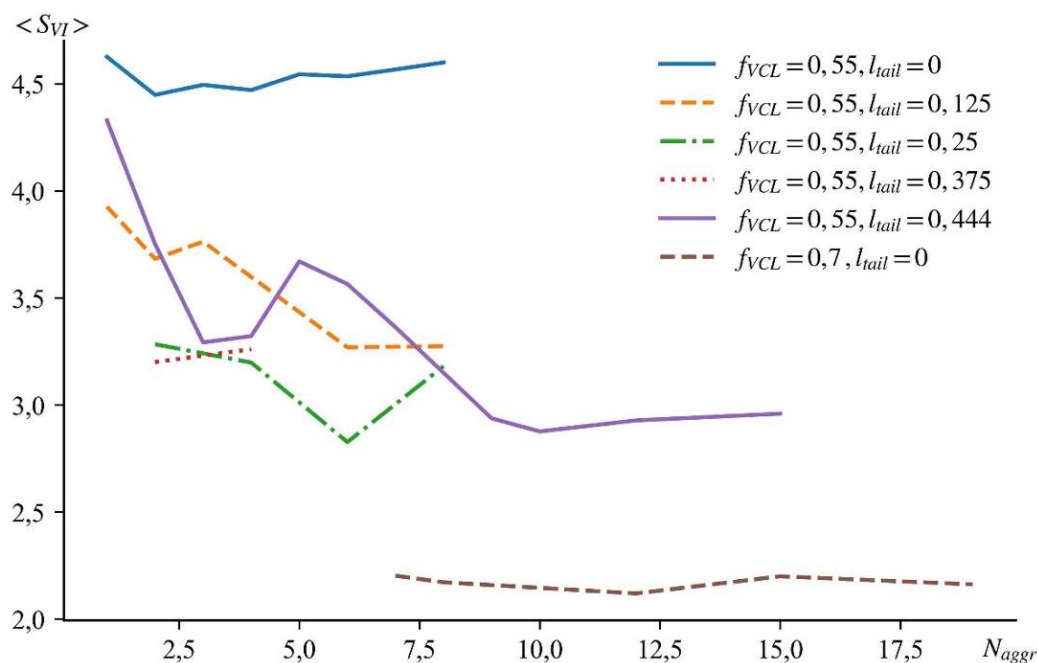


Fig. 3. Average solvent-accessible area per VI unit for aggregates obtained at $f_{VCL} = 0,55$, with $l_{tail} = 0$ (a) and $l_{tail} = 0,45$ (b)

The values of S_{VI} for systems with $f_{VCL} = 0,55$ and $l_{tail} > 0$ are between 2,8 and 4,3, and generally decrease with the increase of both l_{tail} and N_{aggr} . It is worth noting that for systems with $l_{tail} > 0,444$, where large unstable aggregates are formed, and the value of S_{VI} does not decrease for $N_{aggr} > 10$. This corroborates the visual observation that sticking of the spherical aggregates together does not alter their structure. For systems with $f_{VCL} = 0,7$ and $l_{tail} = 0$, the values of S_{VI} are around 2,2 and are virtually independent of the aggregate size. The obtained value is close to the one expected for a dense layer of VI units. Therefore, the polymers obtained at $f_{VCL} = 0,55$ have the highest accessibility of the VI units to the solvent. At the same time, the independence of the S_{VI} on the aggregate size in the systems with $f_{VCL} = 0,7$ allows us to assume that these systems are also aggregation-stable in the considered conditions.

It is known that the metal atoms can coordinate with the N -vinylimidazole units, forming a bond with the nitrogen atom of the imidazole ring. Specifically, the copper ions can coordinate 3 [25] or 4 [12], [13], [14], [26] imidazole monomers, with the geometry of copper (II) atoms in these complexes characterized as distorted square planar [27]. The efficiency of VI -containing catalytic systems can also be augmented by selective adsorption of the substrate on the polymer-solvent boundary [28]. This allows us to assume that the systems with $S_{VI} > 2$ are the most promising as catalysts, because they correspond to the most favorable conditions for the coordination of the metal atoms and contact with the substrate molecules.

5. Conclusions

The aggregation behavior of thermosensitive copolymers based on *N*-vinylcaprolactam and *N*-vinylimidazole was studied by means of computer simulation. The virtual synthesis of the copolymers was implemented using a Kinetic Monte-Carlo model. At low monomer conversion ratios, the statistical copolymers with alteration of *VCL* and *VI* blocks of random lengths were obtained. At higher conversions, the copolymers contained a homopolymer block formed by less reactive *VCL* units. The length of the homopolymer block was controlled by the time at which the reaction was stopped.

The conformational behavior of the macromolecules in the poor solvent for the *VCL* units was studied using Langevin dynamics. The conditions corresponded to the aqueous solvent at temperatures above the lower critical solution temperature for the *VCL*. For all of the solitary chains, the aggregation resulted in the formation of structures with the *VCL* core and the *VI* shell. The presence of a homopolymer *VCL* block led to the formation of a denser core, with short *VCL* blocks within the statistical block of the copolymer adhering to it. The size of the *VI* corona decreased with the increase of the *VCL* content in the monomer feed.

To study the aggregation stability of the obtained nanostructures, they were cloned to build supercells containing 8 or 27 polymer chains in a poor solvent for the *VCL* units. It was found that the polymer synthesized at the lowest *VCL* content in the monomer feed ($f_{VCL} = 0,55$) forms the most stable nanostructures, containing 2-3 polymer chains. These aggregates could reversibly stick together. All nanostructures obtained at the highest *VCL* content $f_{VCL} = 0,85$ formed a single aggregate, pointing to macroscopic phase segregation between the polymer and the solvent. At the intermediate *VCL* content ($f_{VCL} = 0,7$) and a short *PVCL* block, the mesoglobules were formed by constant sets of 12-15 chains. The assessment of the solvent-accessible surface area of the *VI* units has shown that the highest value is observed in the copolymers synthesized at $f_{VCL} = 0,55$. This allows us to consider them as a basis for prospective thermo-switchable catalytic systems. The obtained results can serve as a guideline for future experimental research.

The research was carried out using the equipment of the shared research facilities of HPC computing resources at Lomonosov Moscow State University [29].

The study was funded by a grant Russian Science Foundation (project no. 25-23-00713, <https://rscf.ru/project/25-23-00713/>). Part of the data processing was performed at the Interlaboratory Computing Center of the Institute of Organoelement Compounds, A.N. Nesmeyanov RAS, supported by the Ministry of Science and Higher Education of the Russian Federation.

References:

1. Png Z.M., Wang C.-G., Yeo J.C.C. et. al. Stimuli-responsive structure–property switchable polymer materials, *Molecular Systems Design & Engineering*, 2023, vol. 8, issue 9, pp. 1097-1129. DOI: 10.1039/D3ME00002H.
2. Anker J.N., Hall W.P., Lyandres O. et. al. Biosensing with plasmonic nanosensors, *Nature Materials*, 2008, vol. 7, issue 6, pp. 442-453. DOI: 10.1038/nmat2162.
3. Mendes P.M. Stimuli-responsive surfaces for bio-applications, *Chemical Society Reviews*, 2008, vol. 37, issue 11, pp. 2512-2529. DOI: 10.1039/b714635n.
4. Zhang Y. Lei F. Qian W. et. al. Designing intelligent bioorthogonal nanozymes: Recent advances of stimuli-responsive catalytic systems for biomedical applications, *Journal of Controlled Release*, 2024, vol. 373, pp. 929-951. DOI: 10.1016/j.jconrel.2024.07.073.
5. Ge Z., Xie D., Chen D. et. al. Stimuli-responsive double hydrophilic block copolymer micelles with switchable catalytic activity, *Macromolecules*, 2007, vol. 40, issue 10, pp. 3538-3546. DOI: 10.1021/ma070550i.
6. Wang B. Liu H.-J. Jiang T.-T. Li Q.-H. Chen Y. Thermo-, and pH dual-responsive poly(N-vinylimidazole): Preparation, characterization and its switchable catalytic activity, *Polymer*, 2014, vol. 55, issue 23, pp. 6036-6043. DOI: 10.1016/j.polymer.2014.09.051.
7. Komarov P.V., Zaborina O.E., Klimova T.P. et. al. Designing artificial enzymes from scratch: Experimental study and mesoscale simulation, *Chemical Physics Letters*, 2016, vol. 661, pp. 219-223. DOI: 10.1016/j.cplett.2016.09.009.
8. Musarurwa H., Tavengwa N.T. Thermo-responsive polymers and advances in their applications in separation science, *Microchemical Journal*, 2022, vol. 179, art. no. 107554, 7 p. DOI: 10.1016/j.microc.2022.107554.
9. Xiao Q., Cui Y., Meng Y. et. al. PNIPAm hydrogel composite membrane for high-throughput adsorption of biological macromolecules, *Separation and Purification Technology*, 2022, vol. 294, art. no. 121224, 10 p. DOI: 10.1016/j.seppur.2022.121224.
10. Yao T., Feng C., Yan H. Current developments and applications of smart polymers based aqueous two-phase systems, *Microchemical Journal*, 2024, vol. 204, art. no. 111170, 9 p. DOI: 10.1016/j.microc.2024.111170.
11. Maeda Y., Yamamoto H., Ikeda I. Effects of ionization of incorporated imidazole groups on the phase transitions of poly(*N*-isopropylacrylamide), poly(*N,N*-diethylacrylamide), and poly(*N*-vinylcaprolactam) in water, *Langmuir*, 2001, vol. 17, issue 22, pp. 6855-6859. DOI:10.1021/la0106438.
12. Gold D.H., Gregor H.P. Metal-polyelectrolyte complexes. VIII. The poly-*N*-vinylimidazole—copper(II) complex, *The Journal of Physical Chemistry*, 1960, vol. 64, issue 10, pp. 1464-1467. DOI: 10.1021/j100839a027.
13. Broekema R.J., Durville P.F.M., Reedijk J., Smit J.A. The coordination chemistry of *N*-vinylimidazole, *Transition Metal Chemistry*, 1982, vol. 7, issue 1, pp. 25-28. DOI: 10.1007/BF00623803.
14. Smirnov V.I., Sinegovskaya L.M., Parshina L.N. et. al. Copper(ii), cobalt(ii), manganese(ii) and nickel(ii) bis(hexafluoroacetylacetonate) complexes with *N*-vinylimidazole, *Mendeleev Communications*, 2020, vol. 30, issue 2, pp 246-248. DOI: 10.1016/j.mencom.2020.03.040.
15. Beletskaya I.P., Khokhlov A.R., Tarasenko E.A., Tyurin V.S. Palladium supported on poly(*N*-vinylimidazole) or poly(*N*-vinylimidazole-co-*N*-vinylcaprolactam) as a new recyclable catalyst for the Mizoroki-Heck reaction, *Journal of Organometallic Chemistry*, 2007, vol. 692, issue 20, pp 4402-4406. DOI: 10.1016/j.jorganchem.2007.06.056.
16. Mitrofanov A.Yu., Murashkina A.V., Barabanova A.I. et. al. Efficient recyclable Cu-catalysts for click reaction and Chan-Lam coupling based on copolymers of *N*-vinylimidazole with *N*-vinylcaprolactam, *Molecular Catalysis*, 2023, vol. 541, art. no. 112915, 12 p. DOI: 10.1016/j.mcat.2023.112915.
17. Vyshivannaya O.V., Parkhomenko E.R., Barabanova A.I. et. al. Thermo- and pH-sensitive behavior of copolymers of *N*-vinylcaprolactam with *N*-vinylimidazole, *Polymer Science Series A.*, 2023, vol. 65, issue 3, pp. 235-245. DOI: 10.1134/S0965545X2370092X.
18. Barabanova A.I., Vorozheykina A.V., Glagolev M.K. et. al. Synthesis and theoretical studies of the conformational behaviour of *N*-vinylcaprolactam/*N*-vinylimidazole copolymers in selective solvent, *Molecular Systems Design & Engineering*, 2024, vol. 9, issue 10, pp. 1017-1022. DOI: 10.1039/D4ME00085D.
19. Kremer K., Grest G.S. Dynamics of entangled linear polymer melts: a molecular-dynamics simulation, *The Journal of Chemical Physics*, 1990, vol. 92, issue 8, pp. 5057-5086. DOI: 10.1063/1.458541.
20. Glagolev M.K., Glagoleva A.A., Vasilevskaya V.V. MOUSE2: Molecular Ordering Utilities for Simulations, Edition 2, *Supercomputing Frontiers and Innovations*, 2023, vol. 10, issue 3, pp. 73-87. DOI: 10.14529/jsfi230307.
21. Shrake A., Rupley J.A. Environment and exposure to solvent of protein atoms. Lysozyme and insulin, *Journal of Molecular Biology*, 1973, vol. 79, issue 2, pp. 351-371. DOI:10.1016/0022-2836(73)90011-9.
22. Khokhlov A.R., Khalatur P.G. Biomimetic sequence design in functional copolymers, *Current Opinion in*

- Solid State and Materials Science*, 2004, vol. 8, issue 1, pp. 3-10. DOI: 10.1016/j.cossms.2003.08.001.
23. Khalatur P.G., Khokhlov A.R., Mologin D.A., Reineker P. Aggregation and counterion condensation in solution of charged proteinlike copolymers: A molecular-dynamics study, *The Journal of Chemical Physics*, 2003, vol. 119, issue 2, pp. 1232-1247. DOI: 10.1063/1.1579683.
24. Baburkin P.O., Komarov P.V., Barabanova A.I. et al. Mesoscopic simulation of the synthesis of enzyme-like catalysts, *Doklady Physical Chemistry*, 2016, vol. 470, issue 1, pp. 129-132. DOI: 10.1134/S0012501616090025.
25. Bukowski M.R., Hile B.L., Figurelli A. et al. Insights into heterogeneous phosphodiester hydrolysis using a simple hydrogel-based copper(II)-imidazole catalyst, *Inorganica Chimica Acta*, 2011, vol. 370, issue 1, pp. 405-410. DOI: 10.1016/j.ica.2011.02.011.
26. Zhang W., Wang H., Shentu B. et al. Aerobic oxidative polymerization of 2,6-dimethylphenol in water with a highly efficient copper(II)-poly(*N*-vinylimidazole) complex catalyst, *Journal of Applied Polymer Science*, 2011, vol. 120, issue 1, pp. 109-115. DOI: 10.1002/app.33088.
27. Andersson M., Hansson Ö., Öhrström L. et al. Vinylimidazole copolymers: coordination chemistry, solubility, and cross-linking as function of Cu²⁺ and Zn²⁺ complexation, *Colloid and Polymer Science*, 2011, vol. 289, issue 12, pp. 1361-1372. DOI: 10.1007/s00396-011-2461-5.
28. Okhapkin I.M., Bronstein L.M., Makhaeva E.E. et al. Thermosensitive Imidazole-Containing Polymers as Catalysts in Hydrolytic Decomposition of *p*-Nitrophenyl Acetate, *Macromolecules*, 2004, vol. 37, issue 21, pp. 7879-7883. DOI: 10.1021/ma0487453.
29. Voevodin V.I., Antonov A., Nikitenko D. et al. Supercomputer Lomonosov-2: large scale, deep monitoring and fine analytics for the user community, *Supercomputing Frontiers and Innovations*, 2019, vol. 6, issue 2, pp. 4-11. DOI:10.14529/jsfi190201.

Библиографический список:

1. **Png, Z.M.** Stimuli-responsive structure–property switchable polymer materials / Z.M. Png, C.-G. Wang, J.C.C. Yeo et al. // *Molecular Systems Design & Engineering*. – 2023. – V. 8. – I. 9. – P. 1097-1129. DOI: 10.1039/D3ME00002H.
2. **Anker, J.N.** Biosensing with plasmonic nanosensors / J.N. Anker, W.P. Hall, O. Lyandres et al. // *Nature Materials*. 2008. – V. 7. – I. 6. – P. 442-453. DOI: 10.1038/nmat2162.
3. **Mendes, P.M.** Stimuli-responsive surfaces for bio-applications. / P.M. Mendes // *Chemical Society Reviews*. 2008. – V. 37. – I. 11. – P. 2512-2529. DOI:10.1039/b714635n.
4. **Zhang, Y.** Designing intelligent bioorthogonal nanozymes: Recent advances of stimuli-responsive catalytic systems for biomedical applications / Zhang Y. Lei F. Qian W. et al. // *Journal of Controlled Release*. – 2024. – V. 373. – P. 929-951. DOI:10.1016/j.jconrel.2024.07.073.
5. **Ge, Z.** Stimuli-responsive double hydrophilic block copolymer micelles with switchable catalytic activity / Z. Ge, D. Xie, D. Chen et al. // *Macromolecules*. – 2007. – V. 40. – I. 10. – P. 3538-3546. DOI: 10.1021/ma070550i.
6. **Wang, B.** Thermo-, and pH dual-responsive poly(*N*-vinylimidazole): preparation, characterization and its switchable catalytic activity / B. Wang, H.-J. Liu, T.-T. Jiang et al. // *Polymer*. – 2014. – V. 55. – I. 23. – P. 6036-6043. DOI: 10.1016/j.polymer.2014.09.051.
7. **Komarov, P.V.** Designing artificial enzymes from scratch: Experimental study and mesoscale simulation / P.V. Komarov, O.E. Zaborina, T.P. Klimova et al. // *Chemical Physics Letters*. – 2016. – V. 661. – P. 219-223. DOI: 10.1016/j.cplett.2016.09.009.
8. **Musarurwa, H.** Thermo-responsive polymers and advances in their applications in separation science / H. Musarurwa, N.T. Tavengwa // *Microchemical Journal*. – 2022. – V. 179. – Art. № 107554. – 7 p. DOI:10.1016/j.microc.2022.107554.
9. **Xiao, Q.** PNIPAm hydrogel composite membrane for high-throughput adsorption of biological macromolecules / Q. Xiao, Y. Cui, Y. Meng et al. // *Separation and Purification Technology*. – 2022. – V. 294. – Art. № 121224. – 10 p. DOI :10.1016/j.seppur.2022.121224.
10. **Yao, T.** Current developments and applications of smart polymers based aqueous two-phase systems / T. Yao, C. Feng, H. Yan // *Microchemical Journal*. – 2024. – V. 204. – Art. № 111170. – 9 p. DOI:10.1016/j.microc.2024.111170.
11. **Maeda, Y.** Effects of ionization of incorporated imidazole groups on the phase transitions of poly(*N*-isopropylacrylamide), poly(*N,N*-diethylacrylamide), and poly(*N*-vinylcaprolactam) in water / Y. Maeda, H. Yamamoto, I. Ikeda // *Langmuir*. – 2001. – V. 17. – I. 22. – P. 6855-6859. DOI: 10.1021/la0106438.
12. **Gold, D.H.** Metal–polyelectrolyte complexes. VIII. The poly-*n*-vinylimidazole-copper (II) complex / D.H. Gold, H.P. Gregor // *The Journal of Physical Chemistry*. – 1960. – V. 64. – I. 10. – P. 1464-1467. DOI:

10.1021/j100839a027.

13. **Broekema, R.J.** The coordination chemistry of N-vinylimidazole / R.J. Broekema, P.F.M. Durville, J. Reedijk, J.A. Smit // *Transition Metal Chemistry*. – 1982. – V. 7. – I. 1. – P. 25-28. DOI:10.1007/BF00623803.

14. **Smirnov, V.I.** Copper(ii), cobalt(ii), manganese(ii) and nickel(ii) bis(hexafluoroacetylacetonate) complexes with N-vinylimidazole / V.I. Smirnov, L.M. Sinegovskaya, L.N. Parshina, et. al. // *Mendeleev Communications*. 2020. – V. 30. – I. 2. – P. 246-248. DOI: 10.1016/j.mencom.2020.03.040.

15. **Beletskaya, I.P.** Palladium supported on poly(N-vinylimidazole) or poly(N-vinylimidazole-co-N-vinylcaprolactam) as a new recyclable catalyst for the Mizoroki-Heck reaction / I.P. Beletskaya, A.R. Khokhlov, E.A. Tarasenko, V.S. Tyurin // *Journal of Organometallic Chemistry*. – 2007. – V. 692. – I. 20. – P. 4402-4406. DOI: 10.1016/j.jorganchem.2007.06.056.

16. **Mitrofanov, A.Yu.** Efficient recyclable Cu-catalysts for click reaction and Chan-Lam coupling based on copolymers of N-vinylimidazole with N-vinylcaprolactam / A.Yu. Mitrofanov, A.V. Murashkina, A.I. Barabanova et. al. // *Molecular Catalysis*. – 2023. – V. 541. – Art. № 112915. – 12 p. DOI: 10.1016/j.mcat.2023.112915.

17. **Vyshivannaya, O.V.** Thermo- and pH-sensitive behavior of copolymers of N-vinylcaprolactam with N-vinylimidazole / O.V. Vyshivannaya, E.R. Parkhomenko, A.I. Barabanova et. al. // *Polymer Science Series A*. – 2023. – V. 65. – I. 3. – P. 235-245. DOI: 10.1134/S0965545X2370092X.

18. **Barabanova, A.I.** Synthesis and theoretical studies of the conformational behaviour of N-vinylcaprolactam/N-vinylimidazole copolymers in selective solvent // A.I. Barabanova, A.V. Vorozheykina, M.K. Glagolev et. al. // *Molecular Systems Design & Engineering*. – 2024. – V. 9. – I. 10. – P. 1017-1022. DOI: 10.1039/D4ME00085D.

19. **Kremer, K.** Dynamics of entangled linear polymer melts: A molecular-dynamics simulation / K. Kremer, G.S. Grest // *The Journal of Chemical Physics*. – 1990. – V. 92. – I. 8. – P. 5057-5086. DOI: 10.1063/1.458541.

20. **Glagolev, M.K.** MOUSE2: Molecular Ordering Utilities for Simulations, Edition 2 / M.K. Glagolev, A.A. Glagoleva, V.V. Vasilevskaya // *Supercomputing Frontiers and Innovations*. – 2023. – V. 10. – I. 3. – P. 73-87. DOI: 10.14529/jsfi230307.

21. **Shrake, A.** Environment and exposure to solvent of protein atoms. Lysozyme and insulin / A. Shrake, J.A. Rupley // *Journal of Molecular Biology*. – 1973. – V. 79. – I. 2. – P. 351-371. DOI:10.1016/0022-2836(73)90011-9.

22. **Khokhlov, A.R.** Biomimetic sequence design in functional copolymers / A.R. Khokhlov, P.G. Khalatur // *Current Opinion in Solid State and Materials Science*. – 2004. – V. 8. – I. 1. – P. 3-10. DOI:10.1016/j.cossms.2003.08.001.

23. **Khalatur, P.G.** Aggregation and counterion condensation in solution of charged proteinlike copolymers: a molecular-dynamics study / P.G. Khalatur, A.R. Khokhlov, D.A. Mologin, P. Reineker // *The Journal of Chemical Physics*. – 2003. – V. 119. – I. 2. – P. 1232-1247. DOI: 10.1063/1.1579683.

24. **Baburkin, P.O.** Mesoscopic simulation of the synthesis of enzyme-like catalysts / P.O. Baburkin, P.V. Komarov, A.I. Barabanova et. al. // *Doklady Physical Chemistry*. – 2016. – V. 470. – I. 1. – P. 129-132. DOI:10.1134/S0012501616090025.

25. **Bukowski, M.R.** Insights into heterogeneous phosphodiester hydrolysis using a simple hydrogel-based copper(II)-imidazole catalyst / M.R. Bukowski, B.L. Hile, A. Figurelli et. al. // *Inorganica Chimica Acta*. – 2011. – V. 370. – I. 1. – P. 405-410. DOI: 10.1016/j.ica.2011.02.011.

26. **Zhang, W.** Aerobic oxidative polymerization of 2,6-dimethylphenol in water with a highly efficient copper(II)-poly(N-vinylimidazole) complex catalyst / W. Zhang, H. Wang, B. Shentu et. al. // *Journal of Applied Polymer Science*. – 2011. – V. 120. – I. 1. – P. 109-115. DOI: 10.1002/app.33088.

27. **Andersson, M.** Vinylimidazole copolymers: coordination chemistry, solubility, and cross-linking as function of Cu²⁺ and Zn²⁺ complexation / M. Andersson, Ö. Hansson, L. Öhrström et. al. // *Colloid and Polymer Science*. – 2011. – V. 289. – I. 12. – P. 1361-1372. DOI: 10.1007/s00396-011-2461-5.

28. **Okhapkin, I.M.** Thermosensitive imidazole-containing polymers as catalysts in hydrolytic decomposition of *p*-nitrophenyl acetate / I.M. Okhapkin, L.M. Bronstein, E.E. Makhaeva et. al. // *Macromolecules*. – 2004. – V. 37. – I. 21. – P. 7879-7883. DOI: 10.1021/ma0487453.

29. **Voevodin, V.I.** Supercomputer Lomonosov-2: large scale, deep monitoring and fine analytics for the user Community / V.I. Voevodin, A. Antonov, D. Nikitenko et. al. // *Supercomputing Frontiers and Innovations*. – 2019. – V. 6. – I. 2. – P. 4-11. DOI: 10.14529/jsfi190201.